Advances in Nano Research, *Vol. 10, No. 2 (2021) 175-189*
DOI: https://doi.org/10.12989/anr.2021.10.2.175

Frequency characteristics and sensitivity analysis of a size-dependent laminated nanoshell

Zuocai Dai[1,2a], Zhiyong Jiang[3], Liang Zhang[*4] and Mostafa Habibi[5,6]

[1]*College of Mechanical and Electrical Engineering, Hunan City University, Yiyang 413002, Hunan, China*
[2]*Key Laboratory Energy monitoring and Edge Computing for Smart City of Hunan Province, Yiyang 413002, Hunan, China*
[3]*Practical Teaching Department, Guilin University of Aerospace Technology, Guilin 541004, Guangxi, China*
[4]*School of Aerospace Engineering, Tsinghua University, Beijing 100084, China*
[5]*Institute of Research and Development, Duy Tan University, Da Nang 550000, Vietnam*
[6]*Faculty of Electrical – Electronic Engineering, Duy Tan University, Da Nang 550000, Vietnam*

(*Received July 25, 2020, Revised December 25, 2020, Accepted December 30, 2020*)

Abstract. In this article, frequency characteristics, and sensitivity analysis of a size-dependent laminated composite cylindrical nanoshell under bi-directional thermal loading using Nonlocal Strain-stress Gradient Theory (NSGT) are presented. The governing equations of the laminated composite cylindrical nanoshell in thermal environment are developed using Hamilton's principle. The thermodynamic equations of the laminated cylindrical nanoshell are obtained using First-order Shear Deformation Theory (FSDT) and Fourier-expansion based Generalized Differential Quadrature element Method (FGDQM) is implemented to solve these equations and obtain natural frequency and critical temperature of the presented model. The novelty of the current study is to consider the effects of bi-directional temperature loading and sensitivity parameter on the critical temperature and frequency characteristics of the laminated composite nanostructure. Apart from semi-numerical solution, a finite element model was presented using the finite element package to simulate the response of the laminated cylindrical shell. The results created from finite element simulation illustrates a close agreement with the semi-numerical method results. Finally, the influences of temperature difference, ply angle, length scale and nonlocal parameters on the critical temperature, sensitivity, and frequency of the laminated composite nanostructure are investigated, in details.

Keywords: finite element method; laminated cylindrical nanoshell; sensitivity analysis; bi-directional thermal loading; FGDQM

1. Introduction

In order to achieve desired thermo-mechanical properties, carbon and its derivatives are accounted as the best choices to reinforce engineering structures. Choosing the scale of reinforcement widely depends on the purpose of the engineer (Abualnour *et al*. 2019, Alimirzaei *et al*. 2019, Belbachir *et al*. 2019, 2020, Draiche *et al*. 2019, Medani *et al*. 2019, Sahla *et al*. 2019). Some composites are consisted of a matrix and macroscale reinforcement such as Carbon Fibers (CF) oriented in specific directions to enrich mechanical performance of the structure. Emam and Eltaher (2016) studied post-buckling and buckling performance of the fiber reinforced Euler beam exposed in hygrothermal environment within the framework of Reddy's theory.

On the other side, reinforcing composites with nanofibers instead of macroscale fibers presents noticeable improvement in the mechanical behavior of the structures. Therefore, many researchers focused on the response of Carbon Nanotubes Reinforced (CNTR) structures (Balubaid *et al*. 2019, Bedia *et al*. 2019, Berghouti *et al*. 2019, Boutaleb *et al*. 2019, Semmah *et al*. 2019, Asghar *et al*. 2020, Hussain *et al*. 2020, Khosravi *et al*. 2020, Matouk *et al*. 2020, Taj *et al*. 2020). Maghamikia and Jam (2011) employed Finite Element Method (FEM) to explore buckling behavior of CNTR annular and circular plate on the basis of Third order Shear Deformation Theory (TSDT). They asserted that critical buckling load obtained by their approach are lower than those obtained according to classical theory as a result of considering shear strain terms. Tahouneh and Yas (2014) applied Differential Quadrature Method (DQM) to study vibration characteristics of two dimensional continuously graded CNTR thick disk resting on an elastic substrate within the framework of elasticity theory. As another study, Tahouneh and Jam (2014) investigated free vibration behavior of through the thickness continuously graded CNTR annular plate resting on an elastic foundation on the basis of elasticity theory and employing DQM. In both studies, the Eshelby-Mori-Tanaka micromechanics is used to approximate effective elastic properties of the composite annular plate. Applying Variational Differential Quadrature Method (VDQM) to the governing equations developed based on the First order Shear Deformation Theory (FSDT), Ansari *et al*. (2017) carried out vibration and buckling analyses of Functionally Graded Carbon Nanotube Reinforced Composite (FG-

*Corresponding author, Ph.D.,
E-mail: zl19@tsinghua.org.cn
[a] Ph.D., E-mail: daizuocai@163.com

ISSN: 2287-237X (Print), 2287-2388 (Online)

CNTRC) annular sector plate surrounded by an elastic substrate and subjected to thermal load. By following the same procedure, Keleshtary *et al*. (2017) explored the large amplitude performance of FG-CNTRC annular plate coupled with piezoelectric layer and resting on elastic substrate. Torabi and Ansari (2017) claimed that it is necessary to develop governing equations of large amplitude vibration of FG-CNTRC annular plate in the form of general asymmetric relations in the presence of initial thermally stress to obtain accurate results. Within the framework of FSDT, Pang *et al*. (2018) utilized artificial spring boundary method to model general boundary conditions at each edge of thick FG-CNTRC annular sector plate in order to study vibration response. Buckling performance of moderately thick FG-CNTRC annular sector plate resting on Pasternak elastic substrate and subjected to shear and in-plane loading is analyzed by Ansari *et al*. (2018) on the basis of TSDT and employing VDQM. Gholami and Ansari (2018) carried out nonlinear resonance analysis of FG-CNTRC annular sector plates excited by transverse harmonic load uniformly distributed through the plate area by employing VDQM in the framework of Reddy's TSDT integrated with von Karman nonlinear strain relations.

Viscoelastic materials show both elastic and viscous behavior simultaneously. The viscoelastic materials with damping property attenuate the mechanical vibration. Linear viscoelasticity is normally appeared as time dependency of material properties. There are many models to describe the viscoelastic behavior such as Maxwell (standard), Kelvin-Voigt, Zener and Boltzmann. Pouresmaeeli *et al*. (2013) studied free vibration response of orthotropic viscoelastic nanoplate resting on viscoelastic foundation based on the nonlocal theory of plates and analytical Navier's method. They came to conclusion that increasing damping coefficient causes the natural frequency to be declined dramatically. Within the framework of nonlocal elasticity theory, Arani *et al*. (2012) employed DQM to explore nonlocal vibration of two-layered graphene sheet resting on visco-Pasternak foundation. The results revealed that the highest and lowest frequencies belong to the systems resting on Pasternak and visco-Winkler foundation, respectively. Dynamic buckling performance of graphene sheet coupled with viscoelastic foundation was investigated by Malican and Sadraee Far (2018) based on FSDT and Mindlin's plate theory and utilizing DQM. Hashemi *et al*. (2015) presented an exact analytical solution to free vibration of viscoelastic graphene sheets resting on visco-Pasternak foundation within the framework of Kirchhoff's plate theory together with nonlocal theory. On the basis of Reddy's theory of plates and applying fourth order runge kutta method, Fan *et al*. (2019) carried out nonlinear forced vibration of GPLR multilayer plates resting on visco-Pasternak foundation exposed to thermal environment. Transverse free vibration characteristics of orthotropic viscoelastic microplate resting on visco-Pasternak foundation was investigated by Jamalpoor *et al*. (2019) based on the modified strain gradient theory incorporated with Kirchhoff's plate theory by employing analytical Navier's method. To be beneficial

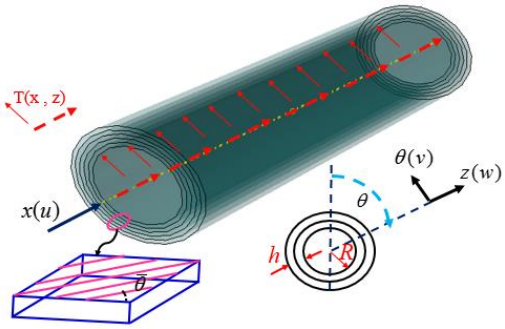

Fig. 1 The geometry of a laminated size-dependent nanoshell under bi-directional thermal loading

of both macro and nano reinforcements, a novel class of composite materials is introduced as Multiscale Hybrid Composites (MHC). The related articles should be classified into three main categories: Those investigate the manufacturing process; those explore the characteristics of MHCs and those related to mechanical behavior of the MHC structures. The article published by Thostenson *et al*. (2002) can be regarded as the primary attempt to obtain multiscale composites with the aid of chemical vapor deposition.

For the first time, the presented study investigates the frequency and thermal buckling analysis of a laminated composite cylindrical nanoshell under bi-directional thermal loading based on NSGT considering the exact values of nonlocal constants and material length scale parameters. The thermodynamic equations of the laminated cylindrical nanoshell are based on FSDT and FGDQM is implemented to solve these equations and obtain natural frequency and critical temperature of the current model. Apart from semi-numerical solution, a finite element model was presented using the finite element package to simulate the response of the smart laminated cylindrical shell. The results created from finite element simulation illustrates a close agreement with the semi-numerical method results. Finally, using the mentioned continuum mechanics theory, the investigation has been made into the influence of the temperature difference, sensitivity and the different types of laminated composites on the critical temperature difference and dynamic stability of the laminated composite nanostructure.

2. Mathematic model

In Fig. 1, a laminated composite cylindrical nanoshell in the thermal environment is sketched. Here h and R are the thickness and the middle surface radius of the nanoshell, respectively. Also, $\bar{\theta}$ is the ply angle of each layer. The material of the nanostructure is considered as a laminated composite.

2.1 Nonlocal strain-stress gradient theory

According to the NSG theory, the general constitutive equation can be expressed as following Eq. (1)

$$(1-\mu^2\nabla^2)t_{ij} = C_{ijck}(1-l^2\nabla^2)\varepsilon_{ck} \quad (1)$$

where, $\nabla^2 = \partial^2/\partial x^2 + \partial^2/R^2\,\partial\theta^2$; t_{ij}, ε_{ck} and C_{ijck} are the components of nonlocal strain gradient stress, strain and elasticity tensors, respectively. Nonlocal strain gradient stress tensor is presented by the following Eq. (2)

$$t_{ij} = \sigma_{ij} - \nabla\sigma_{ij}^{(1)} \quad (2)$$

where σ_{ij} and $\sigma_{ij}^{(1)}$ presented the components of classical and size-dependent stresses, respectively. The μ and l are constants which stand for the impact of non-invariant and higher-order strain gradient stress fields. The calibrated values of the size-dependent parameters are determined by previous experimental studies. The strain tensor is written as

$$\varepsilon_{ij} = \frac{1}{2}\left(u_{i,j} + u_{j,i}\right) \quad (3)$$

where u_i stands for the components of the displacement vector. According to Eq. (3), the stress-strain relation can be presented as Eq. (1).

$$\begin{aligned}&(1-\mu^2\nabla^2)\begin{bmatrix}t_{xx}\\ t_{\theta\theta}\\ t_{x\theta}\end{bmatrix}\\ &= (1-l^2\nabla^2)\begin{bmatrix}C_{11} & C_{12} & 0\\ C_{12} & C_{22} & 0\\ 0 & 0 & C_{66}\end{bmatrix}^{(L)}\begin{bmatrix}\varepsilon_{xx}-\alpha\Delta T\\ \varepsilon_{\theta\theta}-\alpha\Delta T\\ \varepsilon_{x\theta}\end{bmatrix},\\ &(1-\mu^2\nabla^2)\begin{bmatrix}t_{\theta z}\\ t_{xz}\end{bmatrix} = (1-l^2\nabla^2)\begin{bmatrix}C_{44} & 0\\ 0 & C_{55}\end{bmatrix}^{(L)}\begin{bmatrix}\varepsilon_{\theta z}\\ \varepsilon_{xz}\end{bmatrix}\end{aligned} \quad (4)$$

In Eq. (4), thermal expansion and temperature differences are notated by α and ΔT, respectively. For laminated composite materials, the components of the elasticity tensor are known as the reduced elastic constants of the orthotropic material corresponding to L^{th} lamina, and are expressed by the following equations

$$\begin{aligned}C_{11} &= (2\Theta_{12}+4\Theta_{44})\cos^2\theta\sin^2\theta + \Theta_{11}\cos^4\theta + \Theta_{22}\sin^4\theta\\ C_{12} &= 0.5\Theta_{12}\left(2\cos^4\theta + 2\sin^4\theta\right) -\\ &\quad (4\Theta_{44}-\Theta_{11}-\Theta_{22})\cos^2\theta\sin^2\theta\\ C_{22} &= (2\Theta_{12}+4\Theta_{44})\cos^2\theta\sin^2\theta + \Theta_{11}\sin^4\theta\\ &\quad + \Theta_{22}\cos^4\theta\\ C_{44} &= \Theta_{55}\sin^4\theta + \Theta_{44}\cos^4\theta\\ C_{55} &= \Theta_{66}\sin^4\theta + \Theta_{55}\cos^4\theta\\ C_{66} &= \Theta_{66}(\sin^2\theta-\cos^2\theta)^2 -\\ &\quad (2\Theta_{12}-\Theta_{11}-\Theta_{22})\cos^2\theta\sin^2\theta\end{aligned} \quad (5)$$

As mentioned earlier, the relations given by Eq. (5) are the stress-strain constitutive relations referred to the lamina's principal material axes x, θ and z for the Lth orthotropic lamina. In Eq. (5), Q_{ij} components are expressed by the following equations (Boussoula *et al*. 2020, Chikr *et al*. 2020, Kaddari *et al*. 2020, Menasria *et al*. 2020, Rahmani *et al*. 2020, Refrafi *et al*. 2020, Tounsi *et al*. 2020, Zine *et al*. 2020)

$$\begin{aligned}&\Theta_{11} = \frac{E_1}{1-\nu_{21}\nu_{12}}, \qquad \Theta_{12} = \frac{E_2\nu_{12}}{1-\nu_{21}\nu_{12}}\\ &\Theta_{22} = \frac{E_2}{1-\nu_{21}\nu_{12}}\\ &\Theta_{66} = G_{12}, \qquad \Theta_{44} = G_{23}, \qquad \Theta_{55} = G_{13}\end{aligned} \quad (6)$$

2.2 Displacement field

With the aid of first shear order deformation theory, the displacement field of a laminated cylindrical nanoshell is expressed by the following equations (Draiche *et al*. 2019, Bourada *et al*. 2020, Bousahla *et al*. 2020, Matouk *et al*. 2020)

$$\begin{aligned}U(x,\theta,z,t) &= u(x,\theta,z) + z\psi_x(x,\theta,t)\\ V(x,\theta,z,t) &= v(x,\theta,z) + z\psi_\theta(x,\theta,t)\\ W(x,\theta,z,t) &= w(x,\theta,t)\end{aligned} \quad (7)$$

As well as that, $u(x, \theta, t)$, $v(x, \theta, t)$ and $w(x, \theta, t)$ indicate the displacements of the neutral surface along x, and θ directions, respectively. $\psi_x(x, \theta, t)$ and $\psi_\theta(x, \theta, t)$ show the rotations of a cross-section around θ and x-directions. Substituting Eq. (7) into Eq. (3), the components of the strain tensor can be extracted by the following equations

$$\begin{aligned}\varepsilon_{xx} &= \frac{\partial u}{\partial x} + z\frac{\partial\psi_x}{\partial x}, \qquad \varepsilon_{\theta\theta} = \frac{1}{R}\frac{\partial v}{\partial\theta} + \frac{z}{R}\frac{\partial\psi_\theta}{\partial\theta} + \frac{w}{R}\\ \varepsilon_{xz} &= \frac{1}{2}\left(\psi_x + \frac{\partial w}{\partial x}\right)\\ \varepsilon_{x\theta} &= \frac{1}{2}\left(\frac{1}{R}\frac{\partial u}{\partial\theta} + \frac{\partial v}{\partial x}\right) + \frac{z}{2}\left(\frac{1}{R}\frac{\partial\psi_x}{\partial\theta} + \frac{\partial\psi_\theta}{\partial x}\right)\\ \varepsilon_{\theta z} &= \frac{1}{2}\left(\psi_\theta + \frac{1}{R}\frac{\partial w}{\partial\theta} - \frac{v}{R}\right)\end{aligned} \quad (8)$$

2.3 Governing equations and boundary conditions

Based on FSDT and the nonlocal strain gradient theory, the governing equations and boundary conditions of the structure can be obtained using the Hamilton principle by the following equation (Ghayesh 2018a, b, c, 2019a, b)

$$\int_{t_1}^{t_2}(\delta K - \delta\Pi_s + \delta\Pi_w)\;dt = 0 \quad (9)$$

Hear, K is the kinetic energy, Π_s is strain energy and Π_w is the work done by external forces. For the composite layer, Fourier heat conduction relation can be formulated as follows

$$\frac{1}{z}\frac{\partial}{\partial z}\left(k_z z\frac{\partial T}{\partial z}\right) + k_x\frac{\partial^2 T}{\partial x^2} = 0 \quad (10)$$

It should be noted that in the current study $k_x = k_z$. Thermal surface boundary conditions are as below

$$\begin{aligned}&T\left(x,\theta,-\frac{h}{2}\right) = T_0(x)\\ &T\left(x,\theta,\frac{h}{2}\right) = 0\\ &T(0,\theta,z) = T(L,\theta,z) = 0\end{aligned} \quad (11)$$

T_o is the temperature at the inner surface. Based on nonlocal strain gradient theory, the kinetic energy is defined as

$$\begin{aligned}&\delta K = (1+\mu^2\nabla^2)\times\\&\int_Z\iint_A \rho\Big\{\Big(\frac{\partial u}{\partial t}+z\frac{\partial \psi_x}{\partial t}\Big)\Big(\frac{\partial}{\partial t}\delta u+z\frac{\partial}{\partial t}\delta\psi_x\Big)+\Big(\frac{\partial v}{\partial t}+z\frac{\partial \psi_\theta}{\partial t}\Big)\\&\Big(\frac{\partial}{\partial t}\delta v+z\frac{\partial}{\partial t}\delta\psi_\theta\Big)+\Big(\frac{\partial w}{\partial t}\Big)\frac{\partial}{\partial t}\delta w\Big\}Rdzdxd\theta\end{aligned} \tag{12}$$

And also, according to nonlocal strain gradient theory (Karami *et al*. 2019a, b), the strain energy is defined as

$$\begin{aligned}\Pi_s &= \frac{1}{2}\iiint_V\Big(\sigma_{ij}\varepsilon_{ij}+\sigma_{ij}^{(1)}\nabla\varepsilon_{ij}\Big)dV \;\Rightarrow\; \delta\Pi_s\\&= \iiint_S t_{ij}\delta\varepsilon_{ij}dV+\iint_A\sigma_{ij}^{(1)}\delta\varepsilon_{ij}\big|\;{}_0^L dS\end{aligned} \tag{13}$$

Substituting Eq. (8) into Eq. (13), the variation of strain energy can be explained by the following equations

$$\begin{aligned}&\delta\Pi_s =\\&\iint_A\Big\{N_{xx}\frac{\partial}{\partial x}\delta u+M_{xx}\frac{\partial}{\partial x}\delta\psi_x+N_{\theta\theta}\Big(\frac{1}{R}\frac{\partial}{\partial\theta}\delta v+\frac{1}{R}\delta w\Big)\\&+\frac{1}{R}M_{\theta\theta}\frac{\partial}{\partial\theta}\delta\psi_\theta+Q_{xz}\Big(\delta\psi_x+\frac{\partial}{\partial x}\delta w\Big)+N_{x\theta}\times\\&\Big(\frac{1}{R}\frac{\partial}{\partial\theta}\delta u+\frac{\partial}{\partial x}\delta v\Big)+M_{x\theta}\Big(\frac{1}{R}\frac{\partial}{\partial\theta}\delta\psi_x+\frac{\partial}{\partial x}\delta\psi_\theta\Big)+\\&+Q_{z\theta}\Big(\delta\psi_\theta+\frac{1}{R}\frac{\partial}{\partial\theta}\delta w-\frac{1}{R}\delta v\Big)\Big\}Rdxd\theta\\&+\int\Big\{N_{xx}^{(1)}\frac{\partial}{\partial x}\delta u+M_{xx}^{(1)}\frac{\partial}{\partial x}\delta\psi_x+N_{\theta\theta}^{(1)}\Big(\frac{1}{R}\frac{\partial}{\partial\theta}\delta v+\frac{1}{R}\delta w\Big)\\&+\frac{1}{R}M_{\theta\theta}^{(1)}\frac{\partial}{\partial\theta}\delta\psi_\theta+Q_{xz}^{(1)}\Big(\delta\psi_x+\frac{\partial}{\partial x}\delta w\Big)+N_{x\theta}^{(1)}\times\\&\Big(\frac{1}{R}\frac{\partial}{\partial\theta}\delta u+\frac{\partial}{\partial x}\delta v\Big)+M_{x\theta}^{(1)}\Big(\frac{1}{R}\frac{\partial}{\partial\theta}\delta\psi_x+\frac{\partial}{\partial x}\delta\psi_\theta\Big)+\\&Q_{\theta z}^{(1)}\Big(\delta\psi_\theta+\frac{1}{R}\frac{\partial}{\partial\theta}\delta w-\frac{1}{R}\delta v\Big)\Big\}\big|\;{}_0^L Rd\theta\end{aligned} \tag{14}$$

where the force and momentum resultants are

$$\begin{aligned}\begin{Bmatrix}N_{xx},N_{\theta\theta},N_{x\theta}\\N_{xx}^{(1)},N_{\theta\theta}^{(1)},N_{x\theta}^{(1)}\end{Bmatrix}&=\int_{-h/2}^{h/2}\begin{Bmatrix}t_{xx},t_{\theta\theta},t_{x\theta}\\\sigma_{xx}^{(1)},\sigma_{\theta\theta}^{(1)},\sigma_{x\theta}^{(1)}\end{Bmatrix}dz\\\begin{Bmatrix}M_{xx},M_{\theta\theta},M_{x\theta}\\M_{xx}^{(1)},M_{\theta\theta}^{(1)},M_{x\theta}^{(1)}\end{Bmatrix}&=\int_{-h/2}^{h/2}\begin{Bmatrix}t_{xx},t_{\theta\theta},t_{x\theta}\\\sigma_{xx}^{(1)},\sigma_{\theta\theta}^{(1)},\sigma_{x\theta}^{(1)}\end{Bmatrix}zdz\\\begin{Bmatrix}Q_{xz},Q_{\theta z}\\Q_{xz}^{(1)},Q_{\theta z}^{(1)}\end{Bmatrix}&=\int_{-h/2}^{h/2}K_s\begin{Bmatrix}t_{xz},t_{\theta z}\\\sigma_{xz}^{(1)},\sigma_{\theta z}^{(1)}\end{Bmatrix}dz\end{aligned} \tag{15}$$

Governing equations for a cylindrical nanoshell based on the FSDT and NSGT are derived substituting Eqs. (12), and (14) into Eq. (9) so integrating by parts as follows

$$\begin{aligned}\delta u:(1+l^2\nabla^2)\Big(N_{xx,x}+\frac{N_{x\theta,\theta}}{R}\Big)\\=(1+\mu^2\nabla^2)\big(I_0u_{,t^2}+I_1\psi_{x,t^2}\big)\end{aligned} \tag{16}$$

$$\begin{aligned}\delta v:(1+l^2\nabla^2)\Big(N_{x\theta,x}+\frac{N_{\theta\theta,\theta}}{R}+\frac{Q_{z\theta}}{R}\Big)\\=(1+\mu^2\nabla^2)\Big(I_0v_{,t^2}+I_1\psi_{\theta,t^2}\Big)\end{aligned} \tag{17}$$

$$\begin{aligned}\delta w:(1+l^2\nabla^2)\Big(Q_{xz,x}+\frac{Q_{z\theta,\theta}}{R}-\frac{N_{\theta\theta}}{R}\\-\frac{(Y_{xx,\theta x}-Y_{\theta\theta,x\theta})}{2R}\Big)=(1+\mu^2\nabla^2)I_0w_{,t^2}\end{aligned} \tag{18}$$

$$\begin{aligned}\delta\psi_x:(1+l^2\nabla^2)\Big(M_{xx,x}+\frac{M_{\theta\theta,\theta}}{R}-Q_{xz}\Big)\\=(1+\mu^2\nabla^2)\big(I_1u_{,t^2}+I_2\psi_{x,t^2}\big)\end{aligned} \tag{19}$$

$$\begin{aligned}\delta\psi_\theta:(1+l^2\nabla^2)\Big(\frac{M_{\theta\theta,\theta}}{R}+M_{x\theta,x}-Q_{z\theta}\Big)\\=(1+\mu^2\nabla^2)\big(I_1v_{,t^2}+I_2\psi_{\theta,t^2}\big)\end{aligned} \tag{20}$$

3. Solution procedure

3.1 Temperature field

To satisfy temperature boundary conditions (Eq. (11)) and using Eq. (10) and by employing the method of separation of variables and the boundary conditions, the temperature distribution is as below

$$\begin{aligned}&T(x,z)=\\&\sum_{n=1}^{\infty}A_n\frac{K_0(\alpha_n z)\,I_0(\frac{h}{2})(\alpha_n)-I_0(\alpha_n z)\,K_0(\frac{h}{2})(\alpha_n)}{I_0\left(\frac{h}{2}\right)(\alpha_n)}\sin\alpha_n x\\&\alpha_n=\frac{n\pi}{L}\end{aligned} \tag{21}$$

where n is circumferential wave number. It should be noted that K_0 and I_0 are Bessel functions. By applying the boundary conditions at $z=-h/2$ have

$$\begin{aligned}&T_0(x)=\\&\sum_{n=1}^{\infty}A_n\frac{K_0(-\frac{h}{2})(\alpha_n)\,I_0(\frac{h}{2})(\alpha_n)-I_0(-\frac{h}{2})(\alpha_n)K_0(\frac{h}{2})(\alpha_n)}{I_0(\frac{h}{2})(\alpha_n)}\sin\alpha_n x\end{aligned} \tag{22}$$

Multiplying Eq. (22) by $\sin\alpha_n x$ and integrating with respect to z from $x=0$ to $x=L$, have

$$\begin{aligned}&A_n=\frac{2}{L}\times\\&\frac{I_0(\frac{h}{2})(\alpha_n)}{K_0(-\frac{h}{2})(\alpha_n)I_0(\frac{h}{2})(\alpha_n)+I_0(\frac{h}{2})(\alpha_n)\,K_0(\frac{h}{2})(\alpha_n)}\int_0^L T_0(x)\sin\alpha_n x dx\end{aligned} \tag{23}$$

Substituting for A_n, the final expression for the temperature distribution is as follows

$$\begin{aligned}&T(x,z)=\frac{2}{L}\times\\&\sum_{n=1}^{\infty}\frac{\begin{matrix}I_0(\alpha_n z)\,K_0(\alpha_n(h/2))\\-K_0(\alpha_n z)\,I_0(\alpha_n(h/2))\end{matrix}}{\begin{matrix}I_0(\alpha_n(-h/2))K_0(\alpha_n(h/2))\\-K_0(\alpha_n(-h/2))I_0(\alpha_n(h/2))\end{matrix}}\sin\alpha_n x\int_0^L T_0(x)\sin\alpha_n x dx\end{aligned} \tag{24}$$

3.2 Semi-numerical solution procedure

One of the best numerical methods which are well known for its accuracy and convergence is the DQM. In this method it is really important which the numbers of seeds

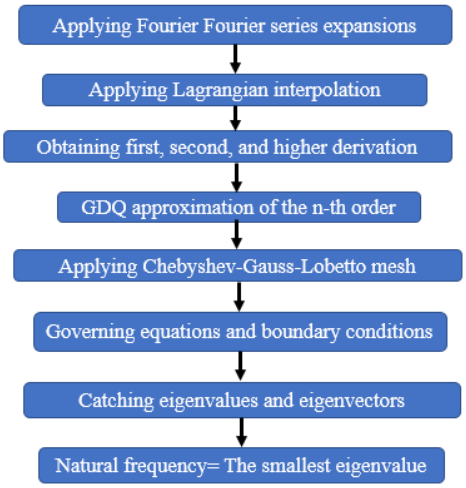

Fig. 2 The flow chart of FGDQM

should be optimal, it means that due to increasing the computational charge, too many seeds are not applicable, on the other hand using the few seeds has a negative effect on result accuracy. At first, this method encounters its users with a limitation which they could not use too many seed owning to the weighting function was algebraic. Shu improved the basic model of DQM with the aid of an explicit formula and decomposition technique so that he renamed the modified method to GDQE. FGDQM is employed with the aim of finding the solutions of governing equations beneath various boundary conditions. The flow chart of this method is in Fig. 2.

With a view of this method estimated r^{th} defined by f(x) as follow.

$$\left.\frac{\partial^r f(x)}{\partial x^r}\right|_{x=x_p} = \sum_{j=1}^{n} C_{ij}^{(r)} f(x_i) \tag{25}$$

n and C_{ij} called the number of seed and weighting coefficients in order which the second one computes as below

$$\begin{aligned} C_{ij}^{(1)} &= \frac{1}{(x_i - x_j)M(x_j)} M(x_i) i \\ j &= 1,2,\ldots,n \quad \text{and} \quad i \neq j \\ C_{ij}^{(1)} &= -\sum_{j=1, i\neq j}^{n} C_{ij}^{(1)} i = j \end{aligned} \tag{26}$$

where

$$M(x_i) = \prod_{j=1, j\neq i}^{n} (x_i - x_j) \tag{27}$$

As well as these higher-order weight coefficients are as follows (Ghabussi *et al*. 2019, Habibi *et al*. 2019, 2020, Al-Furjan *et al*. 2020a-n, Ebrahimi *et al*. 2020, Lori *et al*. 2020, Moayedi *et al*. 2020a, b, Oyarhossein *et al*. 2020, Safarpour *et al*. 2020, Shokrgozar *et al*. 2020).

$$\begin{aligned} C_{ij}^{(r)} &= r\left[C_{ij}^{(r-1)} C_{ij}^{(1)} - \frac{C_{ij}^{(r-1)}}{(x_i - x_j)}\right] i \\ j &= 1,2,\ldots,n, \quad i \neq j \quad \text{and} \quad 2 \leq r \leq n-1 \\ C_{ii}^{(r)} &= -\sum_{j=1, i\neq j}^{n} C_{ij}^{(r)} i \\ j &= 1,2,\ldots,n \quad \text{and} \quad 1 \leq r \leq n-1 \end{aligned} \tag{28}$$

In the present study, a non-uniform set of seeds is selected along with x and θ directions as follows

$$x_i = \frac{L}{2}\left(1 - cos\left(\frac{(i-1)}{(N_i - 1)}\pi\right)\right) i = 1,2,3,\ldots,N_i \tag{29}$$

For simply supported end conditions along circumferential direction, displacements are expressed in terms of Fourier series expansions as follows

$$\begin{aligned} u(x,\theta,t) &= U(x)\cos(n\theta)e^{i\omega t} \\ v(x,\theta,t) &= V(x)\sin(n\theta)e^{i\omega t} \\ w(x,\theta,t) &= W(x)\cos(n\theta)e^{i\omega t} \\ \psi_x(x,\theta,t) &= \Psi_x(x)\cos(n\theta)e^{i\omega t} \\ \psi_\theta(x,\theta,t) &= \Psi_\theta(x)\sin(n\theta)e^{i\omega t} \end{aligned} \tag{30}$$

Reorganizing the quadrature analogs of field equations and boundary conditions inside the fabric of a generalized eigenvalue problem yield

$$\left\{\begin{bmatrix} [M_{dd}] & [M_{db}] \\ [M_{bd}] & [M_{bb}] \end{bmatrix}\omega^2 + \begin{bmatrix} [K_{dd}] & [K_{db}] \\ [K_{bd}] & [K_{bb}] \end{bmatrix}\right\}\begin{Bmatrix} \delta_d \\ \delta_b \end{Bmatrix} = 0 \tag{31}$$

where the subscripts b and d advert to the boundary and domain grid points, respectively. As well as this, δ is the displacement vector. Eq. (31) can be transformed to a standard eigenvalue problem

$$\begin{aligned} [K^\zeta]\{\delta_i\} &= (\omega^2)[M^\zeta]\{\delta_i\} \\ [K^\zeta] &= -[K_{db}{K_{bb}}^{-1}K_{bd} - K_{dd}] \\ [M^\zeta] &= -[M_{db}{K_{bb}}^{-1}K_{bd} - M_{dd}] \end{aligned} \tag{32}$$

As well as this, dimensionless natural frequency and dimensionless temperature difference are defined as below

$$\Omega = 10 \times \omega L\left(\sqrt{\frac{\rho}{E}}\right) \tag{33}$$

$$\Delta\bar{T} = \Delta T\alpha \tag{34}$$

3.3 Sensitivity analysis

In this section, the sensitivity of natural frequency to temperature gradient would be explored. To this end, the sensitivity of i^{th} natural frequency of the MHCAP to temperature gradient is defined as

$$S_i = 100\left(\frac{f_i - f_i^0}{f_i^0}\right) \tag{35}$$

where f_i and f_i^0 indicate the corresponding natural

Table 1 The material properties of AS/3501 graphite-epoxy layers

E_1	E_2	G_{12}	G_{13}	G_{23}	α_1	α_2	v_s
140 GPa	10 GPa	7 GPa	7 GPa	7 GPa	$-0.3 \times 10^{-6}/K$	$28 \times 10^{-6}/K$	0.078

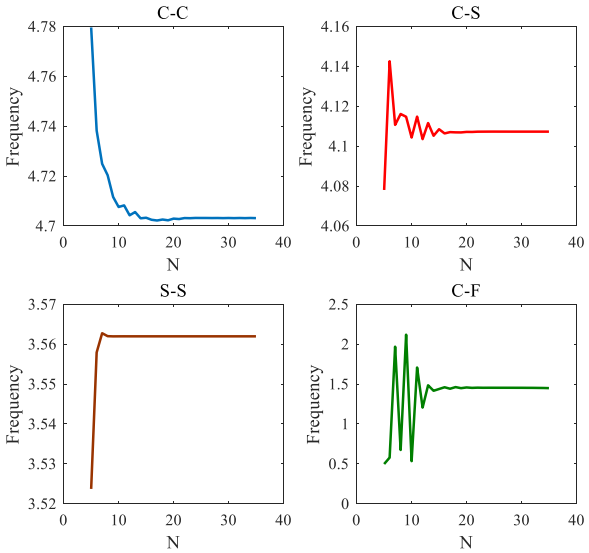

Fig. 3 Influence of the grid points number on the results convergency for the dimensionless frequency of the laminated composites nanoshell for various boundary conditions

frequency of the i^{th} mode number with and without including the effect of temperature gradient, respectively.

4. Result

In this paper, the material properties of the laminated composite cylindrical nanoshell are summarized in Table 1. The main advantages of AS/3501 composite over other existing composites are their high strength and stiffness combined with low density, allowing weight reduction in a finished part and applicable for any parts which work in a thermal environment.

4.1 Convergence study

The sufficient number of grid points is necessary to achieve accurate results in the FGDQM. The convergence studies are conducted for different boundary conditions as well as different materials. Moreover, it can be seen that the structure with C-C boundary conditions is stiffer than the structure with C-F boundary conditions which will lead to a smaller dimensionless critical temperature. According to Fig. 3, for results convergence, twenty grid points are suitable.

4.2 Validation

For results verification of this work with other articles, Table 2 gives a comparison of results for dimensionless

Table 2 Comparison of dimensionless first three natural frequencies of the homogeneous nanoshells, with different length scale parameters

n	Tadi *et al*. (2016) (l = 0)	Present (l = 0)	Tadi *et al*. (2016) (h)	Present (l = h)
1	0.1954	0.19536215	0.1955	0.19543206
2	0.2532	0.25271274	0.2575	0.25731258
3	0.2772	0.27580092	0.3067	0.30621690
1	0.1959	0.19542305	0.1963	0.19585782
2	0.2623	0.25884786	0.2869	0.28543902
3	0.3220	0.31407326	0.4586	0.45457555

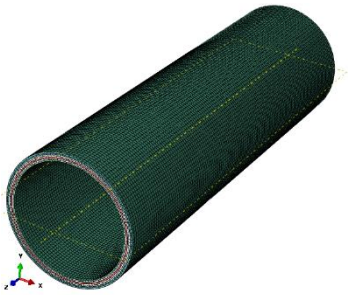

Fig. 4 Meshed FEM laminated shell model

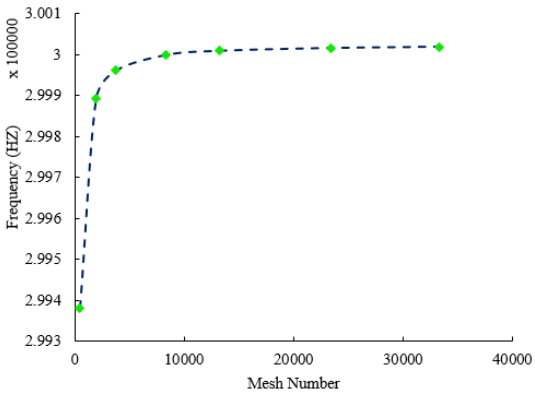

Fig. 5 Mesh convergency for the FE laminated shell model

natural frequency of the cylindrical nanoshell with the results of Tadi Beni *et al*. (2016), for different geometrical parameters. Moreover, the results reveal that the decrease of dimensionless length scale parameter (h/l) would lead to the reduction of the dimensionless natural frequency. In order to validate the proposed formulation, some comparative studies are conducted between the obtained results in this study and those available in the literature. Table 2 shows that there is a very good agreement between the results.

4.3 FEM outcomes

For further validation and shape mode analysis of the shell, finite element analyses have been presented with the aid of ABAQUS, where shell elements (S4R) with a 4-node doubly curved thin or thick shell, reduced integration, hourglass control, finite membrane strains are used to create

Table 3 Validation of numerical results with finite element outcomes

	Numerical results for $N_L = 3$	FEM results for $N_L = 3$	Numerical results for $N_L = 4$	FEM results for $N_L = 4$	Numerical results for $N_L = 5$	FEM results for $N_L = 5$	Numerical results for $N_L = 6$	FEM results for $N_L = 6$
C-C	$1.496e^7$	$1.435e^7$	$2.766e^7$	$2.596e^7$	$2.179e^7$	$2.108e^7$	$2.870e^7$	$2.756e^7$
C-S	$1.271e^7$	$1.205e^7$	$2.003e^7$	$1.912e^7$	$1.620e^7$	$1.520e^7$	$2.071e^7$	$2.003e^7$
S-S	$1.200e^7$	$1.111e^7$	$1.469e^7$	$1.32e^7$	$1.316e^7$	$1.296e^7$	$1.479e^7$	$1.402e^7$
C-F	$7.1327e^6$	$7.020e^6$	$1.196e^7$	$1.100e^7$	$1.006e^7$	$9.859e^6$	$1.249e^7$	$1.119e^7$

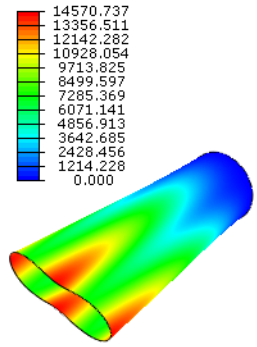

(a) mode: [0 90 0 90 0], (0, 2)

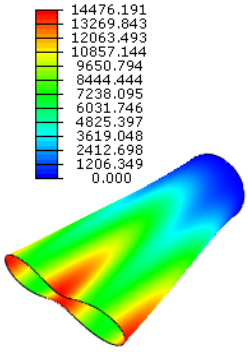

(b) mode: [0 90 0], (0, 2)

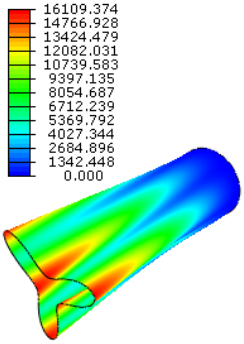

(c) mode: [0 90 0 90 0], (0, 3)

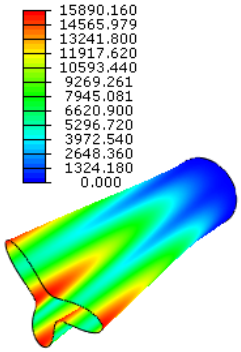

(d) mode: [0 90 0], (0 ,3)

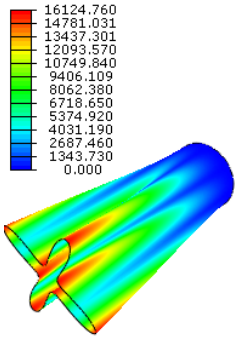

(e) mode: [0 90 0 90 0], (0, 4)

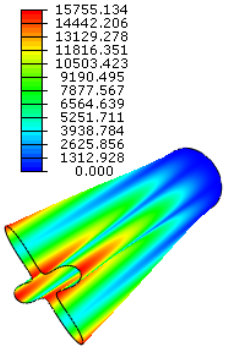

(f) mode: [0 90 0], (0, 4)

Fig. 6 Investigation of the circumferential mode shape of the clamped-free laminated shell with respect to the effect of number of layers

mesh for the shell model. Besides, the perfect bonding between neighboring layers has been considered and Fig. 4 is the model after meshing. In addition, boundary conditions are applied to the nodes at the two edges of the laminated shell. Eventually, the Lanczos eigensolver is presented to obtain the buckling modes and corresponding eigenvalues.

The vector of displacement for the eight-node element S4R would be formulated as

$$\{\delta\} = (u, v, w)^T = \sum_{i=1}^{4} [N_i]\{\delta_i\} \tag{36}$$

where u_i, v_i and w_i are the node displacements i, and the shape function of the node is presented as $[N_i]$. Then element strain vector in the system of global coordinate would be formulated as

$$\{\varepsilon^e\} = \sum_{i=1}^{4} [B_i]\{\delta_i\} \tag{37}$$

where

$$[B_i] = [\Delta][N_i] \tag{38}$$

and Ghabussi *et al*. (2019, 2020a, b), Jermsittiparsert *et al*. (2020), Ma *et al*. (2020), Moayedi *et al*. (2020), Safarpour *et al*. (2020), Shariati *et al*. (2020).

$$[\Delta] = \begin{bmatrix} \partial_{,x} & 0 & 0 \\ 0 & \partial_{,y} & 0 \\ 0 & 0 & \partial_{,z} \\ 0 & \frac{\partial_{,x}}{2} & \frac{\partial_{,z}}{2} \\ \frac{\partial_{,z}}{2} & 0 & \frac{\partial_{,x}}{2} \\ \frac{\partial_{,y}}{2} & \frac{\partial_{,x}}{2} & 0 \end{bmatrix} \tag{39}$$

Also, the stress and strain vectors of an element would be formulated as

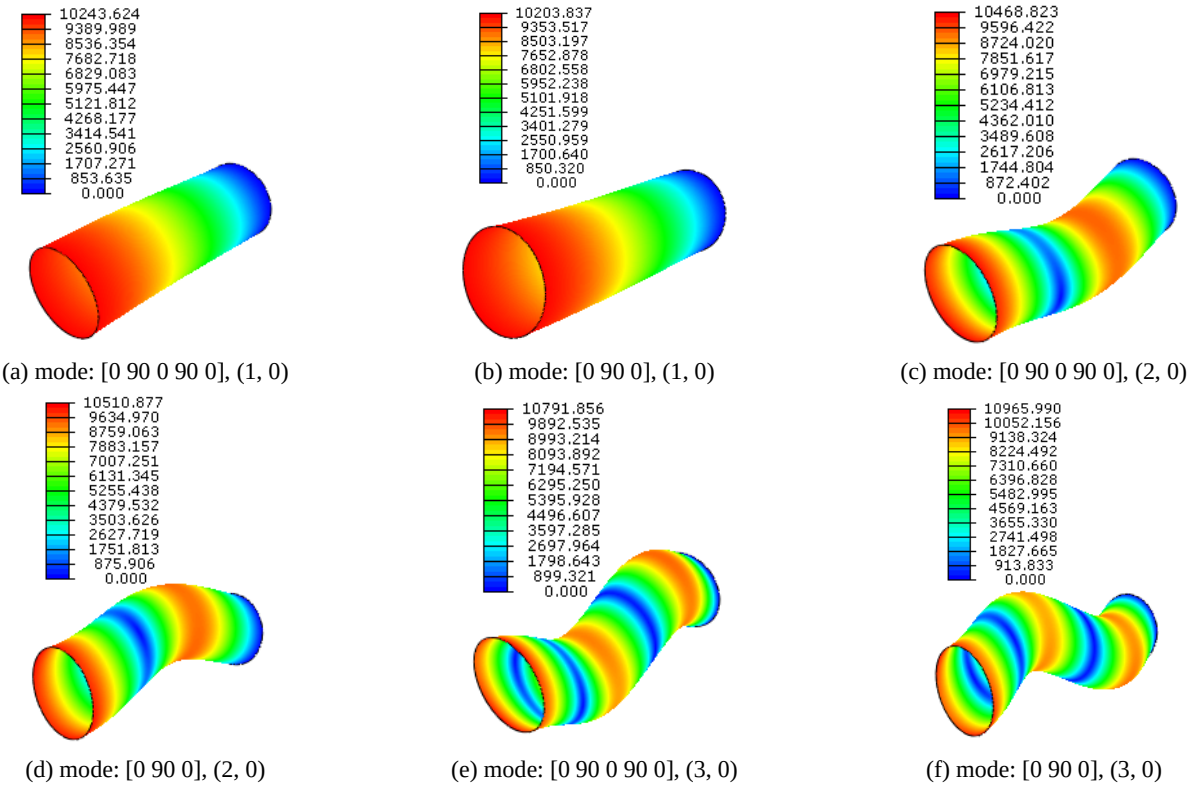

(a) mode: [0 90 0 90 0], (1, 0) (b) mode: [0 90 0], (1, 0) (c) mode: [0 90 0 90 0], (2, 0)

(d) mode: [0 90 0], (2, 0) (e) mode: [0 90 0 90 0], (3, 0) (f) mode: [0 90 0], (3, 0)

Fig. 7 Investigation of the longitudinal mode shape of the clamped-free laminated shell with respect to the effect of number of layers

$$\{\varepsilon^e\} = [B]\{\delta^e\} \tag{40}$$

where $[B] = [B_1 \dots B_8]$, $\{\delta^e\} = \{\{\delta_1\}^T, \dots, \{\delta_8\}^T\}^T$ and $[A]$ indicates matrix transforming local coordinates into global coordinates and $[C]$ presents the elastic constant. Also, the matrix of stiffness ($[K_e]$) can be expressed as

$$[K^e] = \int_{V_e} [B]^T [A][B]^{-1}[B]dV \tag{41}$$

Then the total structure stiffness matrix can be formulated as

$$[K] = \sum_e [K^e] \tag{42}$$

The matrix of mass in the system of global coordinate would be determined as

$$[M] = \sum_e [M^e] \tag{43}$$

and the external force can be expressed as

$$[F] = \sum_e [F^e] \tag{44}$$

By using the minimum potential energy principle, the governing equation can be formulated as

$$\{\delta\}[K] - \{\ddot{\delta}\}[M] = [F] \tag{45}$$

After applying static bending, Eq. (45) can be presented as follows

$$\{\delta\}[K] = [F] \tag{46}$$

Also, the equation of the harmonic free vibration is as below (Ghabussi *et al*. 2019, 2020a, b, Jermsittiparsert *et al*. 2020, Ma *et al*. 2020, Moayedi *et al*. 2020, Safarpour *et al*. 2020, Shariati *et al*. 2020).

$$([K] - \omega^2[M])\{\delta\} = 0 \tag{47}$$

It is well known that if we want to have an accurate FE model we should pay attention to the mesh convergency. For this matter, the number of elements is increased as long as the natural frequency of the structure does not have any change and the optimum number of elements is selected. According to Fig. 5, the convergence condition appears when there are more than 13,000 elements.

Validation study between the numerical results and finite element outcomes is presented in Table 3. As is seen, the maximum relative discrepancies between the numerical and FEM result is less than 4%. In addition, with respect to Table 3 can see that the best pattern in the frequency issue of the structure is N_t = 6 and the more rigid the structure will be a reason for boosting the frequency of the smart shell

In Figs. 6 and 7 we tried to study the effect of number of layers on the circumferential and longitudinal mode shape of the clamped-free laminated shell. Accordingly, can be seen that by increasing the number of layers, the deflection

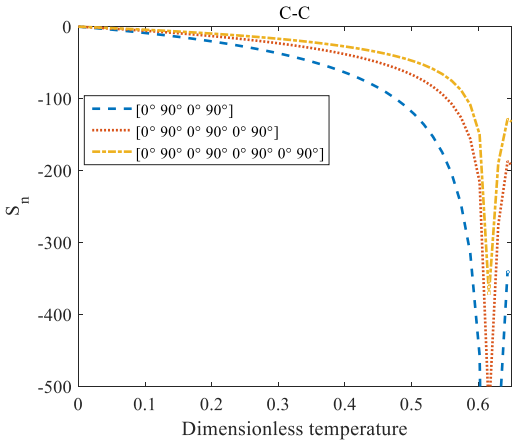

Fig. 8 The effects of dimensionless temperature and even layers number on the sensitivity parameter for C-C boundary conditions

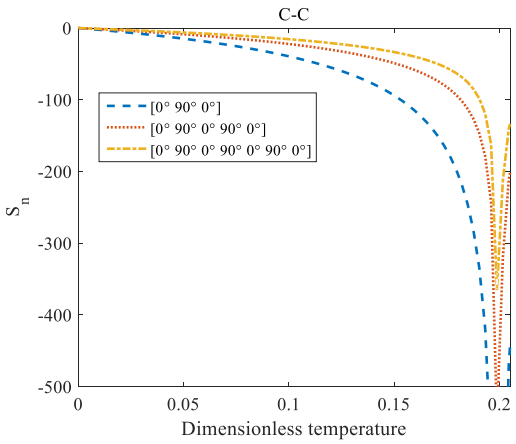

Fig. 11 The effects of dimensionless temperature and odd layers number on the sensitivity parameter for C-C boundary conditions

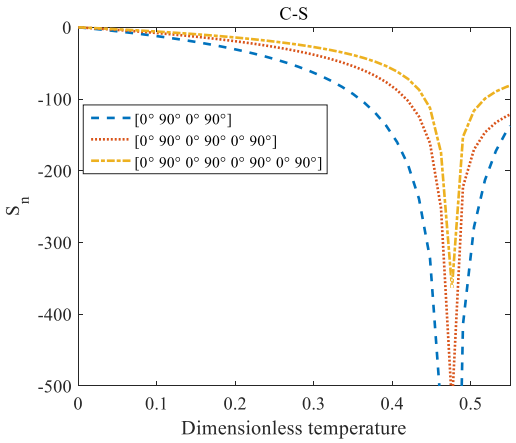

Fig. 9 The effects of dimensionless temperature and even layers number on the sensitivity parameter for C-S boundary conditions

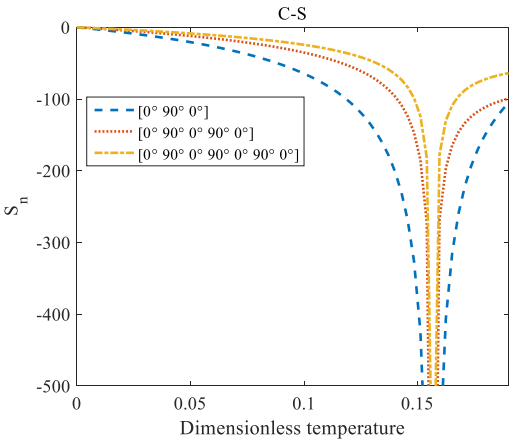

Fig. 12 The effects of dimensionless temperature and odd layers number on the sensitivity parameter for S-S boundary conditions

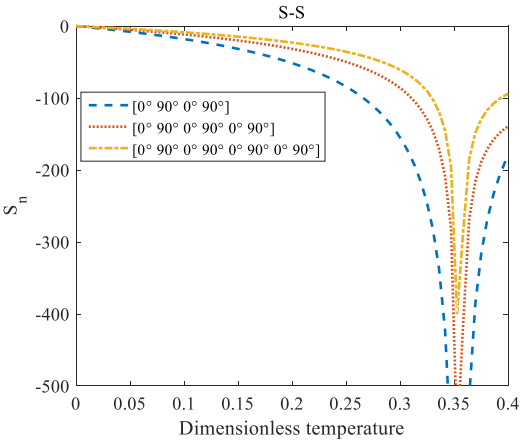

Fig. 10 The effects of dimensionless temperature and even layers number on the sensitivity parameter for S-S boundary conditions

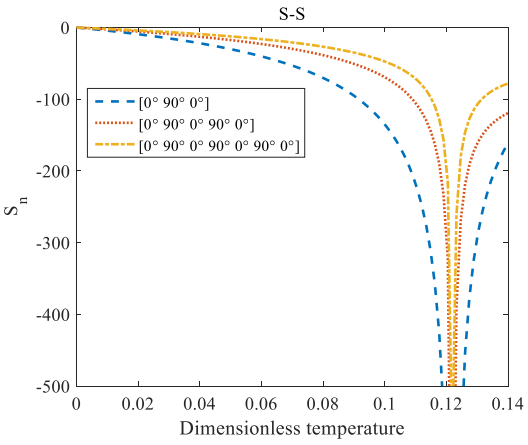

Fig. 13 The effects of dimensionless temperature and odd layers number on the sensitivity parameter for S-S boundary conditions

in the structure will increase and this matter is as a fact in all circumferential and longitudinal mode. Also, the deformation at the free adge can intensified as the number of layers in the laminated shell is decreased.

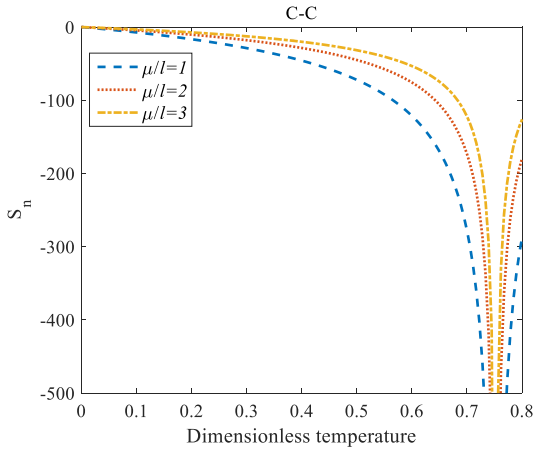

Fig. 14 The effects of μ/l and temperature changes of the environment on the sensitivity of a laminated nanoshell for C-C boundary conditions with L/R = 10, N_t = 3 and n = 1

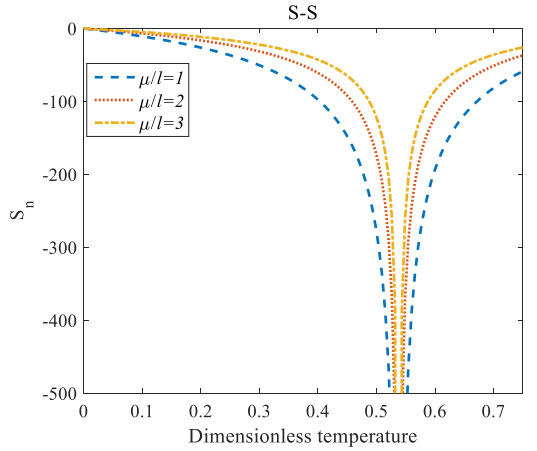

Fig. 16 The effects of of μ/l and temperature changes of the environment on the sensitivity of a laminated nanoshell for S-S boundary conditions with L/R = 10, N_t = 3 and n = 1

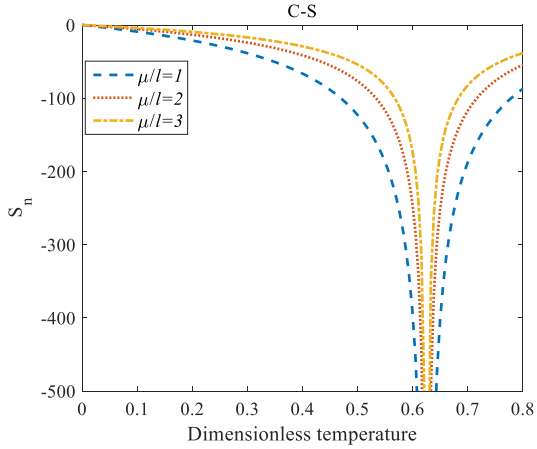

Fig. 15 The effects of of μ/l and temperature changes of the environment on the sensitivity of a laminated nanoshell for C-S boundary conditions with L/R=10, N_t = 3, and n = 1

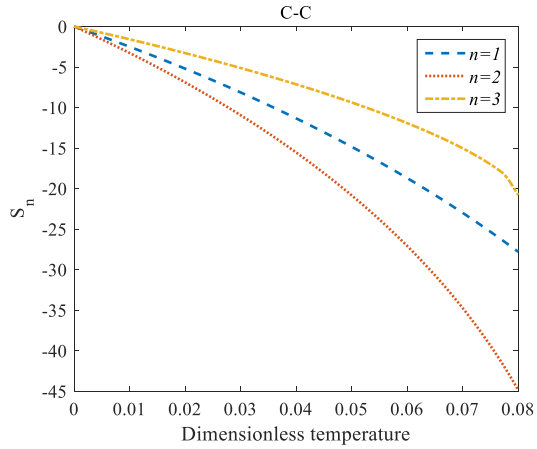

Fig. 17 The effect of temperature rising on the sensitivity analysis of a laminated nanoshell with S-S boundary conditions for L/R = 10 and N_t = 3

4.4 Sensitivity analysis of vibration

According to Figs. 8-10, for C-C, C-S and S-S boundary conditions, a similar relation can find between dimensionless temperature and sensitivity parameter of a laminated nanoshell. As a common outcome, by increasing the dimensionless temperature, the sensitivity parameter of the nanostructure decreases. These figures present that, by boosting the even layers' number of the laminated composite, the absolute value of the sensitivity of the nanostructure decreases and This phenomenon is remarkable for C-C boundary conditions. As the best result for literature, it is seen that increase in the even layers' number doesn't have any effect on the critical temperature for each boundary condition. The difference between Figs. 8, 9 and 10 is that the sensitivity parameter and critical temperature of the C-C boundary condition is higher than other boundary conditions. This is because C-C boundary condition improves the structure stability. As a novel result for literature, increasing the number of laminated layers does not lead to have any effects on the critical temperature of the laminated nanostructure. By having detailed attention to the figures, can claim that when the number of laminated layers is increased, the critical temperature of the nano structure could be seen at the lower value of the sensitivity parameter.

The dimensionless frequency versus the nonlocal parameter for different odd layers number of the laminated composite and S-S, C-S, C-C and C-F boundary conditions are depicted in Figs. 11, 12 and 13. As mentioned earlier, by increasing the dimensionless temperature, the sensitivity parameter is decreased. This decrease is more significant in C-C boundary conditions. The difference between these figures is that the effects of odd layers' number on the sensitivity parameter of the nanostructure with C-C boundary conditions are much more than in comparison with other boundary conditions. As the best result for literature, it is seen that increase in the odd layers' number

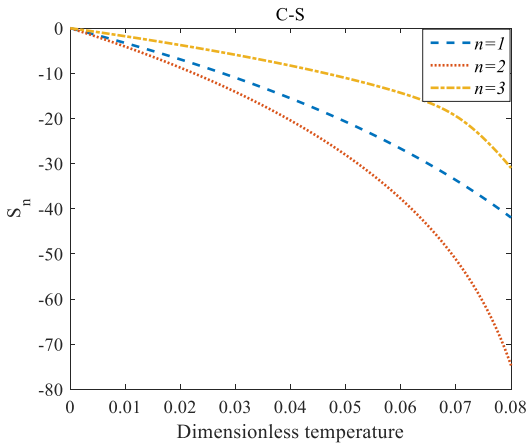

Fig. 18 The effect of temperature rising on the sensitivity analysis of a laminated nanoshell with C-S boundary conditions for L/R = 10 and N_t = 3

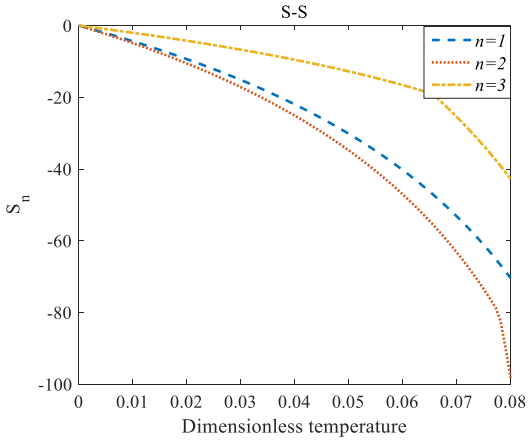

Fig. 19 The effect of temperature rising on the sensitivity analysis of a laminated nanoshell with S-S boundary conditions for L/R = 10 and N_t = 3

doesn't have any effect on the critical temperature for each boundary condition. It can be concluded from the results that temperature difference has a significant effect on the dynamic behavior of the laminated composite nanostructure.

Figs. 14, 15 and 16 present the effect of dimensionless size-dependent parameter (μ/l) on the S_n parameter with different boundary conditions. It can be observed that by increasing temperature, the dynamic stability of the nanostructure has been decreased as long as critical temperature is seen. As the best result for literature, it is seen that increase in the μ/l doesn't have any effects on the critical temperature for each boundary condition. Also, it is concluded that the absolute value of sensitivity for μ/l = 1 is higher than other dimensionless size dependent parameters in an equal temperature difference. The difference between Figs. 14, 15 and 16 is that, for a specific value of the μ/l, the critical temperature of C-C boundary conditions is higher than S-S and C-S boundary conditions. It is clear from these figures; nonlocal parameter doesn't show any effects on the critical temperature of the laminated cylindrical nanoshell. By having an exact glance to the Figs. 14, 15 and 16, for each boundary conditions can find out the impact of μ/l parameter on the S_n is considerable at the lowe value of the temperature gradiant.

The sensitivity of the natural frequency as function of temperature for different circumferential wave number and boundary conditions are computed and presented in Figs. 17, 18 and 19. The displayed results in the figure illustrate that the absolute values of frequency sensitivity increase by increasing the temperature gradient. Also, it is concluded that the absolute value of sensitivity for second circumferential mode number is remarkable than other circumferential mode numbers in an equal temperature difference. The effect of circumferential mode numbers and temperature gradient on the sensitivity response is considerable when these relations are investigated at the higher value of the dimensionless temperature.

5. Conclusions

This article investigated the sensitivity, thermal buckling and stability analysis of a size-dependent laminated composite cylindrical nanoshell under bi-directional thermal loading using NSGT. In the current study and for the first time, the sensitivity, critical temperature and dynamic stability analysis of a laminated composite cylindrical nanoshell under bi-directional thermal loading are examined based on an exact continuum theory. the investigation has been made into the influence of the temperature difference and the different types of laminated composite on the sensitivity, and vibrational characteristics of the nanostructure. In this work, the following main results have been achieved.

• By increasing the number of layers, the deflection in the structure will increase and this matter is as a fact in all circumferential and longitudinal mode

• By boosting the number of layers, the amplitude of the shell doesn't have any changes when the circumferential mode number is one.

• For C-C, C-S and S-S boundary conditions and every even and odd layers' number, by increasing the length scale parameter and layers' number, the frequency of the structure increases.

• The absolute value of sensitivity for μ/l = 1 is higher than other dimensionless size dependent parameters in an equal temperature difference.

The number of layers has a positive effect on the critical temperature of the laminated composite cylindrical nanoshell.

Acknowledgments

This work was supported by the Project of Key Laboratory Energy monitoring and Edge Computing for Smart City of Hunan Province (No.2017TP1024), the Scientific Research project of Hunan Education Department

(20B113), the Teaching Reform Research Project of Hunan City university (202024), the Curriculum ideological and political education reform of College of Mechanical and Electrical Engineering (202015).

References

Abualnour, M., Chikh, A., Hebali, H., Kaci, A., Tounsi, A., Bousahla, A.A. and Tounsi, A. (2019), "Thermomechanical analysis of antisymmetric laminated reinforced composite plates using a new four variable trigonometric refined plate theory", *Comput. Concrete, Int. J.*, **24**(6), 489-498. https://doi.org/10.12989/cac.2019.24.6.489.

Al-Furjan, M., Alzahrani, B., Shan, L., Habibi, M. and Jung, D.W. (2020a), "Nonlinear forced vibrations of nanocomposite-reinforced viscoelastic thick annular system under hygrothermal environment", *Mech. Based Des. Struct. Mach.*, **2020**, 1-27. https://doi.org/10.1080/15397734.2020.1824795.

Al-Furjan, M., Bolandi, S.Y., Shan, L., Habibi, M. and Jung, D.W. (2020b), "On the vibrations of a high-speed rotating multi-hybrid nanocomposite reinforced cantilevered microdisk", *Mech. Based Des. Struct. Mach.*, **2020**, 1-29. https://doi.org/10.1080/15397734.2020.1828098.

Al-Furjan, M., Fereidouni, M., Habibi, M., Abd Ali, R., Ni, J. and Safarpour, M. (2020c), "Influence of in-plane loading on the vibrations of the fully symmetric mechanical systems via dynamic simulation and generalized differential quadrature framework", *Eng. Comput.*, **2020**, 1-23. https://doi.org/10.1007/s00366-020-01177-7.

Al-Furjan, M., Habibi, M. and Safarpour, H. (2020d), "Vibration control of a smart shell reinforced by graphene nanoplatelets", *Int. J. Appl. Mech.*, **12**(6), 2050066. https://doi.org/10.1142/S1758825120500660.

Al-Furjan, M., Habibi, M., Chen, G., Safarpour, H., Safarpour, M. and Tounsi, A. (2020e), "Chaotic oscillation of a multi-scale hybrid nano-composites reinforced disk under harmonic excitation via GDQM", *Compos. Struct.*, **252**, 112737. https://doi.org/10.1016/j.compstruct.2020.112737.

Al-Furjan, M., Habibi, M., Chen, G., Safarpour, H., Safarpour, M. and Tounsi, A. (2020f), "Chaotic oscillation of a multi-scale hybrid nano-composites reinforced disk under harmonic excitation via GDQM", *Compos. Struct.*, **2020**, 112737. https://doi.org/10.1016/j.compstruct.2020.112737.

Al-Furjan, M., Habibi, M., Chen, G., Safarpour, H., Safarpour, M. and Tounsi, A. (2020g), "Chaotic simulation of the multi-phase reinforced thermo-elastic disk using GDQM", *Eng. Comput.*, **2020**, 1-24. https://doi.org/10.1007/s00366-020-01144-2.

Al-Furjan, M., Habibi, M., Jung, D.W., Chen, G., Safarpour, M. and Safarpour, H. (2020h), "Chaotic responses and nonlinear dynamics of the graphene nanoplatelets reinforced doubly-curved panel", *Eur. J. Mech. A Solids*, **2020**, 104091. https://doi.org/10.1016/j.euromechsol.2020.104091.

Al-Furjan, M., Habibi, M., Jung, D.W., Sadeghi, S., Safarpour, H., Tounsi, A. and Chen, G. (2020i), "A computational framework for propagated waves in a sandwich doubly curved nanocomposite panel", *Eng. Comput.*, **2020**, 1-18. https://doi.org/10.1007/s00366-020-01130-8.

Al-Furjan, M., Mohammadgholiha, M., Alarifi, I.M., Habibi, M. and Safarpour, H. (2020j), "On the phase velocity simulation of the multi curved viscoelastic system via an exact solution framework", *Eng. Comput.*, **2020**, 1-17. https://doi.org/10.1007/s00366-020-01152-2.

Al-Furjan, M., Oyarhossein, M.A., Habibi, M., Safarpour, H. and Jung, D.W. (2020k), "Frequency and critical angular velocity characteristics of rotary laminated cantilever microdisk via two-dimensional analysis", *Thin-Wall. Struct.*, **157**, 107111. https://doi.org/10.1016/j.tws.2020.107111.

Al-Furjan, M., Oyarhossein, M.A., Habibi, M., Safarpour, H. and Jung, D.W. (2020l), "Wave propagation simulation in an electrically open shell reinforced with multi-phase nanocomposites", *Eng. Comput.*, **2020**, 1-17. https://doi.org/10.1007/s00366-020-01167-9.

Al-Furjan, M., Oyarhossein, M.A., Habibi, M., Safarpour, H., Jung, D.W. and Tounsi, A. (2020m), "On the wave propagation of the multi-scale hybrid nanocomposite doubly curved viscoelastic panel", *Compos. Struct.*, **2020**, 112947. https://doi.org/10.1016/j.compstruct.2020.112947.

Al-Furjan, M., Safarpour, H., Habibi, M., Safarpour, M. and Tounsi, A. (2020n), "A comprehensive computational approach for nonlinear thermal instability of the electrically FG-GPLRC disk based on GDQ method", *Eng. Comput.*, **2020**, 1-18. https://doi.org/10.1007/s00366-020-01088-7.

Alimirzaei, S., Mohammadimehr, M. and Tounsi, A. (2019), "Nonlinear analysis of viscoelastic micro-composite beam with geometrical imperfection using FEM: MSGT electro-magneto-elastic bending, buckling and vibration solutions", *Struct. Eng. Mech., Int. J.*, **71**(5), 485-502. https://doi.org/10.12989/sem.2019.71.5.485.

Ansari, R., Torabi, J. and Shojaei, M.F. (2017), "Buckling and vibration analysis of embedded functionally graded carbon nanotube-reinforced composite annular sector plates under thermal loading", *Compos. Part B Eng.*, **109**, 197-213. https://doi.org/10.1016/j.compositesb.2016.10.050.

Ansari, R., Torabi, J. and Hassani, R. (2018), "In-plane and shear buckling analysis of FG-CNTRC annular sector plates based on the third-order shear deformation theory using a numerical approach", *Comput. Math. Appl.*, **75**(2), 486-502. https://doi.org/10.1016/j.camwa.2017.09.022.

Arani, A.G., Shiravand, A., Rahi, M. and Kolahchi, R. (2012), "Nonlocal vibration of coupled DLGS systems embedded on visco-Pasternak foundation", *Physica B Condens. Matter.*, **407**(21), 4123-4131. https://doi.org/10.1016/j.physb.2012.06.035.

Asghar, S., Naeem, M.N., Hussain, M., Taj, M. and Tounsi, A. (2020), "Prediction and assessment of nonlocal natural frequencies of DWCNTs: Vibration analysis", *Comput. Concrete, Int. J.*, **25**(2), 133-144. https://doi.org/10.12989/cac.2020.25.2.133.

Balubaid, M., Tounsi, A., Dakhel, B. and Mahmoud, S. (2019), "Free vibration investigation of FG nanoscale plate using nonlocal two variables integral refined plate theory", *Comput. Concrete, Int. J.*, **24**(6), 579-586. https://doi.org/10.12989/cac.2019.24.6.579.

Bedia, W.A., Houari, M.S.A., Bessaim, A., Bousahla, A.A., Tounsi, A., Saeed, T. and Alhodaly, M.S. (2019), "A new hyperbolic two-unknown beam model for bending and buckling analysis of a nonlocal strain gradient nanobeams", *J. Nano Res.*, **57**, 175-191. https://doi.org/10.4028/www.scientific.net/JNanoR.57.175.

Belbachir, N., Draich, K., Bousahla, A.A., Bourada, M., Tounsi, A. and Mohammadimehr, M. (2019), "Bending analysis of anti-symmetric cross-ply laminated plates under nonlinear thermal and mechanical loadings", *Steel Compos. Struct.*, **33**(1), 81-92. https://doi.org/10.12989/scs.2019.33.1.081.

Belbachir, N., Bourada, M., Draiche, K., Tounsi, A., Bourada, F., Bousahla, A.A. and Mahmoud, S. (2020), "Thermal flexural analysis of anti-symmetric cross-ply laminated plates using a four variable refined theory", *Smart Struct. Syst., Int. J.*, **25**(4), 409-422. https://doi.org/10.12989/sss.2020.25.4.409.

Berghouti, H., Adda Bedia, E., Benkhedda, A. and Tounsi, A. (2019), "Vibration analysis of nonlocal porous nanobeams made of functionally graded material", *Adv. Nano Res., Int. J.*, **7**(5), 351-364. https://doi.org/10.12989/anr.2019.7.5.351.

Bourada, F., Bousahla, A.A., Tounsi, A., Bedia, E., Mahmoud, S., Benrahou, K.H. and Tounsi, A. (2020), "Stability and dynamic analyses of SW-CNT reinforced concrete beam resting on elastic-foundation", *Comput. Concrete, Int. J.*, **25**(6), 485-495. https://doi.org/10.12989/cac.2020.25.6.485.

Bousahla, A.A., Bourada, F., Mahmoud, S., Tounsi, A., Algarni, A., Bedia, E. and Tounsi, A. (2020a), "Buckling and dynamic behavior of the simply supported CNT-RC beams using an integral-first shear deformation theory", *Comput. Concrete, Int. J.*, **25**(2), 155-166. https://doi.org/10.12989/cac.2020.25.2.155.

Boussoula, A., Boucham, B., Bourada, M., Bourada, F., Tounsi, A., Bousahla, A.A. and Tounsi, A. (2020b), "A simple nth-order shear deformation theory for thermomechanical bending analysis of different configurations of FG sandwich plates", *Smart Struct. Syst., Int. J.*, **25**(2), 197-218. https://doi.org/10.12989/sss.2020.25.2.197.

Boutaleb, S., Benrahou, K.H., Bakora, A., Algarni, A., Bousahla, A.A., Tounsi, A., Tounsi, A. and Mahmoud, S. (2019), "Dynamic analysis of nanosize FG rectangular plates based on simple nonlocal quasi 3D HSDT", *Adv. Nano Res., Int. J.*, **7**(3), 191-208. https://doi.org/10.12989/anr.2019.7.3.191.

Chikr, S.C., Kaci, A., Bousahla, A.A., Bourada, F., Tounsi, A., Bedia, E., Mahmoud, S., Benrahou, K.H. and Tounsi, A. (2020), "A novel four-unknown integral model for buckling response of FG sandwich plates resting on elastic foundations under various boundary conditions using Galerkin's approach", *Geomech. Eng., Int. J.*, **21**(5), 471-487. https://doi.org/10.12989/gae.2020.21.5.471.

Draiche, K., Bousahla, A.A., Tounsi, A., Alwabli, A.S., Tounsi, A. and Mahmoud, S. (2019), "Static analysis of laminated reinforced composite plates using a simple first-order shear deformation theory", *Comput. Concrete, Int. J.*, **24**(4), 369-378. https://doi.org/10.12989/cac.2019.24.4.369.

Ebrahimi, F., Supeni, E.E.B., Habibi, M. and Safarpour, H. (2020), "Frequency characteristics of a GPL-reinforced composite microdisk coupled with a piezoelectric layer", *Eur. Phys. J. Plus.* **135**(2), 144. https://doi.org/10.1140/epjp/s13360-020-00217-x.

Emam, S. and Eltaher, M. (2016), "Buckling and postbuckling of composite beams in hygrothermal environments", *Compos. Struct.*, **152** 665-675. https://doi.org/10.1016/j.compstruct.2016.05.029.

Fan, Y., Xiang, Y. and Shen, H.S. (2019), "Nonlinear forced vibration of FG-GRC laminated plates resting on visco-Pasternak foundations", *Compos. Struct.*, **209**, 443-452. https://doi.org/10.1016/j.compstruct.2018.10.084.

Ghabussi, A., Ashrafi, N., Shavalipour, A., Hosseinpour, A., Habibi, M., Moayedi, H., Babaei, B. and Safarpour, H. (2019), "Free vibration analysis of an electro-elastic GPLRC cylindrical shell surrounded by viscoelastic foundation using modified length-couple stress parameter", *Mech. Based Des. Struct. Mach.*, **2019**, 1-25. https://doi.org/10.1080/15397734.2019.1705166.

Ghabussi, A., Habibi, M., NoormohammadiArani, O., Shavalipour, A., Moayedi, H. and Safarpour, H. (2020a), "Frequency characteristics of a viscoelastic graphene nanoplatelet-reinforced composite circular microplate", *J. Vib. Control*, **2020**, 1077546320923930. https://doi.org/10.1177/1077546320923930.

Ghabussi, A., Marnani, J.A. and Rohanimanesh, M.S. (2020b), "Improving seismic performance of portal frame structures with steel curved dampers", *Structures*, **24**, 27-40. https://doi.org/10.1016/j.istruc.2019.12.025.

Ghayesh, M.H. (2018a), "Dynamics of functionally graded viscoelastic microbeams", *Int. J. Eng. Sci.*, **124**, 115-131. https://doi.org/10.1016/j.ijengsci.2017.11.004.

Ghayesh, M.H. (2018b), "Functionally graded microbeams: simultaneous presence of imperfection and viscoelasticity", *Int. J. Eng. Sci.*, **140**, 339-350. https://doi.org/10.1016/j.ijmecsci.2018.02.037.

Ghayesh, M.H. (2018c), "Nonlinear vibration analysis of axially functionally graded shear-deformable tapered beams", *Appl. Math. Model.*, **59**, 583-596. https://doi.org/10.1016/j.apm.2018.02.017.

Ghayesh, M.H. (2019a), "Viscoelastic dynamics of axially FG microbeams", *Int. J. Eng. Sci.*, **135**, 75-85. https://doi.org/10.1016/j.ijengsci.2018.10.005.

Ghayesh, M.H. (2019b), "Viscoelastic mechanics of Timoshenko functionally graded imperfect microbeams", *Compos. Struct.*, **225**, 110974. https://doi.org/10.1016/j.compstruct.2019.110974.

Gholami, R. and Ansari, R. (2018), "Geometrically nonlinear resonance of higher-order shear deformable functionally graded carbon-nanotube-reinforced composite annular sector plates excited by harmonic transverse loading", *Eur. Phys. J. Plus*, **133**(2), 1-18. https://doi.org/10.1140/epjp/i2018-11874-6.

Habibi, M., Mohammadi, A., Safarpour, H., Shavalipour, A. and Ghadiri, M. (2019), "Wave propagation analysis of the laminated cylindrical nanoshell coupled with a piezoelectric actuator", *Mech. Based Des. Struct. Mach.*, **2019**, 1-19. https://doi.org/10.1080/15397734.2019.1697932.

Habibi, M., Safarpour, M. and Safarpour, H. (2020), "Vibrational characteristics of a FG-GPLRC viscoelastic thick annular plate using fourth-order Runge-Kutta and GDQ methods", *Mech. Based Des. Struct. Mach.*, **2020**, 1-22. https://doi.org/10.1080/15397734.2020.1779086.

Hashemi, S.H., Mehrabani, H. and Ahmadi-Savadkoohi, A. (2015), "Exact solution for free vibration of coupled double viscoelastic graphene sheets by viscoPasternak medium", *Compos. Part B Eng.*, **78**, 377-383. https://doi.org/10.1016/j.compositesb.2015.04.008.

Hussain, M., Naeem, M.N., Taj, M. and Tounsi, A. (2020), "Simulating vibration of single-walled carbon nanotube using Rayleigh-Ritz's method", *Adv. Nano Res., Int. J.*, **8**(3), 215-228. https://doi.org/10.12989/anr.2020.8.3.215.

Jamalpoor, A., Bahreman, M. and Hosseini, M. (2019), "Free transverse vibration analysis of orthotropic multi-viscoelastic microplate system embedded in visco-Pasternak medium via modified strain gradient theory", *J. Sandw. Struct. Mater.*, **21**(1), 175-210. https://doi.org/10.1177/1099636216689384.

Jermsittiparsert, K., Ghabussi, A., Forooghi, A., Shavalipour, A., Habibi, M., Jung, D.W. and Safa, M. (2020), "Critical voltage, thermal buckling and frequency characteristics of a thermally affected GPL reinforced composite microdisk covered with piezoelectric actuator", *Mech. Based Des. Struct. Mach.*, **2020**, 1-23. https://doi.org/10.1080/15397734.2020.1748052.

Kaddari, M., Kaci, A., Bousahla, A.A., Tounsi, A., Bourada, F., Tounsi, A., Bedia, E. and Al-Osta, M.A. (2020), "A study on the structural behaviour of functionally graded porous plates on elastic foundation using a new quasi-3D model: Bending and free vibration analysis", *Comput. Concrete, Int. J.*, **25**(1), 37-57. https://doi.org/10.12989/cac.2020.25.1.037.

Karami, B., Janghorban, M. and Tounsi, A. (2019a), "Galerkin's approach for buckling analysis of functionally graded anisotropic nanoplates/different boundary conditions", *Eng. Comput.*, **35**(4), 1297-1316. https://doi.org/10.1007/s00366-018-0664-9.

Karami, B., Janghorban, M. and Tounsi, A. (2019b), "On pre-stressed functionally graded anisotropic nanoshell in magnetic field", *J. Braz. Soc. Mech. Sci. Eng.*, **41**(11), 495. https://doi.org/10.1007/s40430-019-1996-0.

Keleshteri, M., Asadi, H. and Wang, Q. (2017), "Large amplitude vibration of FG-CNT reinforced composite annular plates with integrated piezoelectric layers on elastic foundation", *Thin-Wall. Struct.*, **120**, 203-214. https://doi.org/10.1016/j.tws.2017.08.035.

Khosravi, F., Hosseini, S.A. and Tounsi, A. (2020), "Forced axial vibration of a single-walled carbon nanotube embedded in elastic medium under various moving forces", *J. Nano Res.*, **62**, 112-133. https://doi.org/10.4028/www.scientific.net/JNanoR.63.112.

Lori, E.S., Ebrahimi, F., Supeni, E.E.B., Habibi, M. and Safarpour, H. (2020), "The critical voltage of a GPL-reinforced composite microdisk covered with piezoelectric layer", *Eng. Comput.*, **2020**, 1-20. https://doi.org/10.1007/s00366-020-01004-z.

Ma, X., Foong, L.K., Morasaei, A., Ghabussi, A. and Lyu, Z. (2020), "Swarm-based hybridizations of neural network for predicting the concrete strength", *Smart Struct. Syst., Int. J.*, **26**(2), 241-251. https://doi.org/10.12989/sss.2020.26.2.241.

Maghamikia, S. and Jam, J. (2011), "Buckling analysis of circular and annular composite plates reinforced with carbon nanotubes using FEM", *J. Mech. Sci. Technol.*, **25**(11), 2805-2810. https://doi.org/10.1007/s12206-011-0738-8.

Malikan, M. and Sadraee Far, M.N. (2018), "Differential quadrature method for dynamic buckling of graphene sheet coupled by a viscoelastic medium using neperian frequency based on nonlocal elasticity theory", *J. Appl. Comput. Mech.*, **4**(3), 147-160. https://doi.org/10.22055/jacm.2017.22661.1138.

Matouk, H., Bousahla, A.A., Heireche, H., Bourada, F., Bedia, E., Tounsi, A., Mahmoud, S., Tounsi, A. and Benrahou, K. (2020), "Investigation on hygro-thermal vibration of P-FG and symmetric S-FG nanobeam using integral Timoshenko beam theory", *Adv. Nano Res., Int. J.*, **8**(4), 293-305. https://doi.org/10.12989/anr.2020.8.4.293.

Medani, M., Benahmed, A., Zidour, M., Heireche, H., Tounsi, A., Bousahla, A.A., Tounsi, A. and Mahmoud, S. (2019), "Static and dynamic behavior of (FG-CNT) reinforced porous sandwich plate using energy principle", *Steel Compos. Struct., Int. J.*, **32**(5), 595-610. https://doi.org/10.12989/scs.2019.32.5.595.

Menasria, A., Kaci, A., Bousahla, A.A., Bourada, F., Tounsi, A., Benrahou, K.H., Tounsi, A., Adda Bedia, E. and Mahmoud, S. (2020), "A four-unknown refined plate theory for dynamic analysis of FG-sandwich plates under various boundary conditions", *Steel Compos. Struct., Int. J.*, **36**(3), 355-367. https://doi.org/10.12989/scs.2020.36.3.355.

Moayedi, H., Aliakbarlou, H., Jebeli, M., Noormohammadiarani, O., Habibi, M., Safarpour, H. and Foong, L. (2020a), "Thermal buckling responses of a graphene reinforced composite micropanel structure", *Int. J. Appl. Mech.*, **12**(1), 2050010. https://doi.org/10.1142/S1758825120500106.

Moayedi, H., Darabi, R., Ghabussi, A., Habibi, M. and Foong, L.K. (2020b), "Weld orientation effects on the formability of tailor welded thin steel sheets", *Thin-Wall. Struct.*, **149**, 106669. https://doi.org/10.1016/j.tws.2020.106669.

Oyarhossein, M.A., Alizadeh, A.A., Habibi, M., Makkiabadi, M., Daman, M., Safarpour, H. and Jung, D.W. (2020), "Dynamic response of the nonlocal strain-stress gradient in laminated polymer composites microtubes", *Sci. Rep.*, **10**(1), 1-19. https://doi.org/10.1038/s41598-020-61855-w.

Pang, F., Li, H., Du, Y., Shan, Y. and Ji, F. (2018), "Free vibration of functionally graded carbon nanotube reinforced composite annular sector plate with general boundary supports", *Curved Layer. Struct.*, **5**(1), 49-67. https://doi.org/10.1515/cls-2018-0005.

Pouresmaeeli, S., Ghavanloo, E. and Fazelzadeh, S. (2013), "Vibration analysis of viscoelastic orthotropic nanoplates resting on viscoelastic medium", *Compos. Struct.*, **96** 405-410. https://doi.org/10.1016/j.compstruct.2012.08.051.

Rahmani, M.C., Kaci, A., Bousahla, A.A., Bourada, F., Tounsi, A., Bedia, E., Mahmoud, S., Benrahou, K.H. and Tounsi, A. (2020), "Influence of boundary conditions on the bending and free vibration behavior of FGM sandwich plates using a four-unknown refined integral plate theory", *Comput. Concrete., Int. J.*, **25**(3), 225-244. https://doi.org/10.12989/cac.2020.25.3.225.

Refrafi, S., Bousahla, A.A., Bouhadra, A., Menasria, A., Bourada, F., Tounsi, A., Bedia, E., Mahmoud, S., Benrahou, K.H. and Tounsi, A. (2020), "Effects of hygro-thermo-mechanical conditions on the buckling of FG sandwich plates resting on elastic foundations", *Comput. Concrete., Int. J.*, **25**(4), 311-325. https://doi.org/10.12989/cac.2020.25.4.311.

Safarpour, M., Ghabussi, A., Ebrahimi, F., Habibi, M. and Safarpour, H. (2020), "Frequency characteristics of FG-GPLRC viscoelastic thick annular plate with the aid of GDQM", *Thin-Wall. Struct.*, **150**, 106683. https://doi.org/10.1016/j.tws.2020.106683.

Sahla, M., Saidi, H., Draiche, K., Bousahla, A.A., Bourada, F. and Tounsi, A. (2019), "Free vibration analysis of angle-ply laminated composite and soft core sandwich plates", *Steel Compos. Struct., Int. J.*, **33**(5), 663-679. https://doi.org/10.12989/scs.2019.33.5.663.

Semmah, A., Heireche, H., Bousahla, A.A. and Tounsi, A. (2019), "Thermal buckling analysis of SWBNNT on Winkler foundation by non-local FSDT", *Adv. Nano Res., Int. J.*, **7**(2), 89-98. https://doi.org/10.12989/anr.2019.7.2.089.

Shariati, A., Ghabussi, A., Habibi, M., Safarpour, H., Safarpour, M., Tounsi, A. and Safa, M. (2020), "Extremely large oscillation and nonlinear frequency of a multi-scale hybrid disk resting on nonlinear elastic foundation", *Thin-Wall. Struct.*, **154**, 106840. https://doi.org/10.1016/j.tws.2020.106840.

Shokrgozar, A., Ghabussi, A., Ebrahimi, F., Habibi, M. and Safarpour, H. (2020), "Viscoelastic dynamics and static responses of a graphene nanoplatelets-reinforced composite cylindrical microshell", *Mech. Based Des. Struct. Mach.*, **2020**, 1-28. https://doi.org/10.1080/15397734.2020.1719509.

Tadi Beni, Y., Mehralian, F. and Zeighampour, H. (2016), "The modified couple stress functionally graded cylindrical thin shell formulation", *Mech. Adv. Mater. Struct.*, **23**(7), 791-801. https://doi.org/10.1080/15376494.2015.1029167.

Tahouneh, V. and Eskandari-Jam, J. (2014), "A semi-analytical solution for 3-D dynamic analysis of thick continuously graded carbon nanotube-reinforced annular plates resting on a two-parameter elastic foundation", *Mech. Adv. Compos. Struct.*, **1**(2), 113-130. https://doi.org/10.22075/macs.2014.286.

Tahouneh, V. and Yas, M. (2014), "Influence of equivalent continuum model based on the Eshelby-Mori-Tanaka scheme on the vibrational response of elastically supported thick continuously graded carbon nanotube-reinforced annular plates", *Polym. Compos.*, **35**(8), 1644-1661. https://doi.org/10.1002/pc.22818.

Taj, M., Majeed, A., Hussain, M., Naeem, M.N., Safeer, M., Ahmad, M., Khan, H.U. and Tounsi, A. (2020), "Non-local orthotropic elastic shell model for vibration analysis of protein microtubules", *Comput. Concrete, Int. J.*, **25**(3), 245-253. https://doi.org/10.12989/cac.2020.25.3.245.

Thostenson, E., Li, W., Wang, D., Ren, Z. and Chou, T. (2002), "Carbon nanotube/carbon fiber hybrid multiscale composites", *J. Appl. Phys.*, **91**(9), 6034-6037. https://doi.org/10.1063/1.1466880.

Torabi, J. and Ansari, R. (2017), "Nonlinear free vibration analysis of thermally induced FG-CNTRC annular plates: Asymmetric versus axisymmetric study", *Comput. Methods Appl. Mech. Eng.*, **324**, 327-347. https://doi.org/10.1016/j.cma.2017.05.025.

Tounsi, A., Al-Dulaijan, S., Al-Osta, M.A., Chikh, A., Al-Zahrani, M., Sharif, A. and Tounsi, A. (2020), "A four variable trigonometric integral plate theory for hygro-thermo-mechanical bending analysis of AFG ceramic-metal plates resting on a two-parameter elastic foundation", *Steel Compos. Struct., Int. J.*, **34**(4), 511-524. https://doi.org/10.12989/scs.2020.34.4.511.

Zine, A., Bousahla, A.A., Bourada, F., Benrahou, K.H., Tounsi, A.,

Adda Bedia, E., Mahmoud, S. and Tounsi, A. (2020), "Bending analysis of functionally graded porous plates via a refined shear deformation theory", *Comput. Concrete, Int. J.*, **26**(1), 63-74. https://doi.org/10.12989/cac.2020.26.1.063.

CC